Photoacoustic spectroscopic study of energy gap, optical absorption, and thermal diffusivity of polycrystalline $ZnSe_xTe_{1-x}$ $(0 \leq x \leq 1)$ alloys

A. K. Ghosh, K. K. Som, S. Chatterjee, and B. K. Chaudhuri
Solid State Physics Department, Indian Association for the Cultivation of Science, Calcutta 700 032, India
(Received 16 May 1994; revised manuscript received 21 September 1994)

Using the photoacoustic spectroscopic (PAS) technique, we report on the results of composition-dependent optical band gap (E_0), absorption coefficient (α), and thermal diffusivity (σ) of the $ZnSe_xTe_{1-x}$ $(0 \leq x \leq 1)$ type alloys. The band gap is found to vary nonlinearly with composition, showing downward bowing with a minimum around $x = 0.32$. Unlike $A^{I}B^{III}C_2^{VI}$ chalcopyrite-structure alloys [Phys. Rev. B **44**, 163 (1991)], the nonlinear variation of E_0 with x for the Zn-Se-Te system cannot be explained by the electronegativity difference between the substituting atoms. However, the gap parameter $E_0(x)$ can be expressed as $E_0(x) = a + bx + cx^2$ (where a, b, and c are real parameters calculated for these alloys). Similar downward bowing is also observed from the concentration-dependent band-edge effective mass (m_e^*) of the carriers (also obtained from the present experimental data) indicating that the bowing is an intrinsic property of the Zn-Se-Te-type materials. The exponential edge (Urbach edge) is observed for these samples. The absorption process can be considered as an internal Franz-Keldysh effect arising due to the phonon-generated electric field. It could be described in the framework of the Dow-Redfield model. The determination of the thermal diffusivity and the phonon-assisted indirect transition at the band tail of these samples are also results for these materials obtained from the present PAS studies.

I. INTRODUCTION

Photoacoustic spectroscopy (PAS) is an important technique for the nondestructive characterization of semiconductors and other materials.[1] The nonradiative absorption processes which are associated with the band structure, defect-related energy loss mechanisms, etc. can be directly and very accurately obtained from analysis of the PAS spectra.[1–5] Since the photoacoustic response of the materials depends only on the absorbed light and not on the transmitted radiation, this technique is also convenient for measuring optical properties of light-absorbing (crystalline or disordered) materials. Moreover, PAS has some advantages[6] over the conventional transmission method, the photocurrent method, and photothermal deflection spectroscopy for use at the low optical-absorption region ($\alpha < 10^3$ cm^{-1}) and at low temperatures. The PAS technique can be employed for both low- and high-temperature[7] spectroscopic studies.

To the best of our knowledge no photoacoustic investigation of the energy band structure, optical-absorption coefficient, etc. of many technologically important semiconducting materials[8–10] like Zn-Se-Te, Zn-S-Te, Zn-S-Se, etc. has so far been made. These materials are very important for many applications in optical and electronic devices.[10,11] However, some other spectroscopic techniques have been used earlier to study the optical properties of some of these materials.[12–15]

Like the optical band gap, the thermal diffusivity σ (defined as $\sigma = k/\rho C$, where k is the thermal conductivity, ρ the mass density, and C the specific heat) is also an important physical parameter not only for its intrinsic physical interest, but also for its use in device modeling and design. Physically, the inverse of σ is a measure of the time required to establish thermal equilibrium for a given sample. The thermal diffusivity, like the optical band gap, is also a unique parameter for each material, but extremely dependent upon the compositional and microstructural variables.[16] Recently the PAS technique has been used by deLima *et al.*[17] to measure the concentration-dependent thermal diffusivity of glassy Ge_xTe_{1-x} materials.

In this paper we present results on the energy gap, thermal diffusivity, and optical-absorption coefficient near the fundamental edge of the $ZnSe_xTe_{1-x}$ $(0 \leq x \leq 1)$ type polycrystalline alloys using a high-resolution photoacoustic spectrometer in the visible spectral region. Unlike many other similar compounds, the Zn-Se-Te system is found to show an interesting nonlinear variation of the energy gap and other related parameters with concentration x.

Our organization of this paper is as follows. In Sec. II we have briefly discussed the method of sample preparation and experimental procedure with the PAS. Section III deals with the experimental results and discussion of the observed band gap, thermal diffusivity, band-edge effective mass, exponential edge, and absorption tail of the prepared samples. The results have also been compared with those obtained from other spectroscopic studies. The paper ends with the summary and conclusion in Sec. IV.

II. EXPERIMENT

The samples like $ZnSe_xTe_{1-x}$ or ZnS_xSe_{1-x} $(0 \leq x \leq 1)$ were prepared from their respective melts. Appropriate amounts of highly pure (99.999%) Zn, Se (or S), and Te (Johnson Matthey) in a vacuum-sealed quartz tube were melted at 1000 °C for about 36 h. The sample tube was occasionally rotated inside the furnace for

thorough mixing of the melt. The ampoule was then furnace cooled to room temperature. The samples thus prepared were polycrystalline lumps and their compositions and structure were tested by x-ray-diffraction studies which were compared with the structural data.[12,14] Energy-dispersive x-ray analysis confirmed that the Zn:Se:Te ratio was in agreement with the mixing ratio.

The single-beam photoacoustic spectrometer used in the present investigation consists of a small-volume gas-microphone PA cell, a 1000-W Xe lamp with power supply (Müller, Germany, type SVX 1000), a monochromator (Oriel model 77250), and a mechanical chopper (SR 540) discussed in our earlier paper.[18] The PA signal produced is detected by a sensitive electrate microphone (Bruel & Kjaer Model: 4147) and processed by using a preamplifier (B.&K. model 2639) and a lock-in amplifier (Stanford Research model SR 530). Thin pellets cut from the lump samples are polished and then they are used for recording the PA absorption spectra. To minimize light scattering[2] from the sample, very thin (3–4 mm diameter and ~0.3 mm thick) samples were used for the present PAS studies. All the spectra were recorded at room temperature using a chopping frequency of 120 Hz, which gives a thermal diffusion length of about 60–70 μm for the Zn-Se-Te samples studied. The optical band gap E_0 is determined by measuring the variation of the normalized PA signal with the wavelength of the incident light. The PA spectrum obtained from highly absorbing carbon-black powder is used to normalize the spectrum obtained for each sample. An IBM personal computer is used for the acquisition and processing of the data from the lock-in amplifier through an RS-232 interface.

III. RESULTS AND DISCUSSION

A. Absorption coefficient and band gap

The normalized PA spectrum of $ZnSe_xTe_{1-x}$ $(0 \le x \le 1)$ as a function of incident photon energy is shown in Fig. 1. The optical-absorption coefficient α for thick samples is calculated[4,19] from the relation

$$\alpha=(1/\mu_s)[q^2+q(2-q^2)^{1/2}]/(1-q^2)\ , \tag{1}$$

where q is the normalized PA signal intensity. μ_s is the thermal diffusion length given by[1]

$$\mu_s=(2\sigma/\omega)^{1/2}=(f_c l_s^2/\pi f)^{1/2}\ , \tag{2a}$$

where $\omega=2\pi f$ (f is the chopping frequency). f_c and l_s are related to the thermal diffusivity σ, obeying the relation[20]

$$\sigma=f_c l_s^2\ , \tag{2b}$$

where l_s is the sample thickness in cm. Since the samples used for our PAS measurements are homogeneous alloys and very thin slices (obtained by cutting and polishing the bulk solid lumps), the use of Eqs. (1) and (2) seems to be quite reasonable. This is also indicated from the agreement of E_0 values obtained from the present PAS studies with those obtained from other spectroscopic techniques.

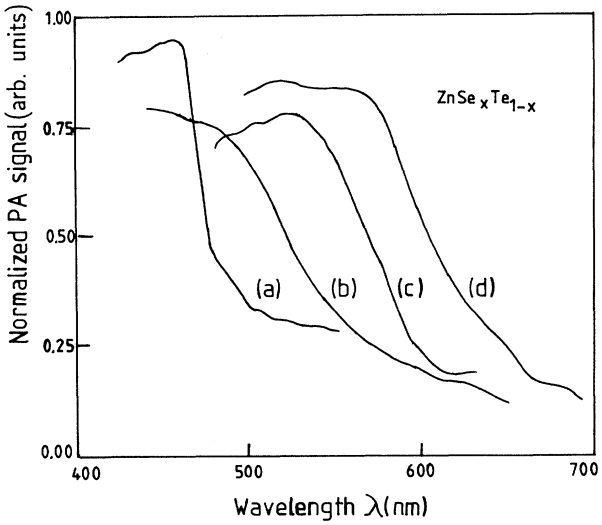

FIG. 1. Normalized photoacoustic spectra of $ZnSe_xTe_{1-x}$, as a function of photon energy, containing information about the optical properties of the samples. Curve *a*, ZnSe, curve *b*, $ZnSe_{0.8}Te_{0.2}$, curve *c*, ZnTe, and curve *d*, $ZnSe_{0.3}Te_{0.7}$.

The samples are called thermally thick when $f > f_c$ and thermally thin when $f < f_c$ [f_c is the characteristic frequency[20,21] at which the sample goes from a thermally thin regime to a thermally thick regime and it is determined from the log-log plots (Fig. 2) of the PA signal amplitude Q_{PA} versus the chopping angular frequency ω]. For $f > f_c$, the PA signal is independent of the thermal properties of the backing materials[20,21] and the plot is parallel to that of the reference sample (thickness ~0.5 mm). For $f < f_c$ the PA amplitude Q_{PA} depends[20] on σ_s as well as on the ratio $g=K_b\sigma_s/K_s\sigma_b$, where subscripts s and b indicate the parameters for the sample and the

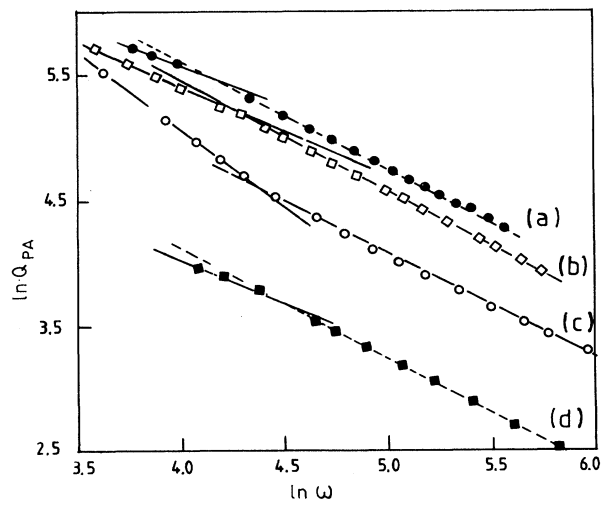

FIG. 2. Logarithmic plots of the photoacoustic signal amplitude Q_{PA} with the chopping angular frequency ω. Curve *a*, $ZnSe_{0.3}Te_{0.7}$, curve *b*, $ZnSe_{0.8}Te_{0.2}$, curve *c*, ZnTe, and curve *d*, ZnSe.

backing materials. $K_{b,s}$ are the thermal conductivities. The plot of $\ln Q_{PA}$ vs $\ln\omega$ as in Fig. 2 indicates a discontinuity at f_c with an increase (for $g<1$ as shown in Fig. 2, curve *c*) or decrease of the slope (for $g>1$ as in Fig. 2, curves *a*, *b*, and *d*). The thermal diffusivity σ obtained from Eq. (2b) is shown in Fig. 3 as a function of concentration x and is found to vary nonlinearly with concentration (Table I). Since no other experimental data of thermal diffusivity σ are available for the Zn-Se-Te system to our knowledge, we cannot compare our results with others. These values of σ are, however, comparable with those of glassy Ge_xTe_{1-x} ($\sigma\sim 2\times10^{-2}$ cm^2/sec, Ref. 17) and As-Se-Te ($\sigma\sim 2\times10^{-2}$ cm^2/sec, Ref. 21) systems.

Figure 4 shows the absorption coefficients α for different samples as a function of the incident photon energy $h\nu$. The absorption spectrum (Fig. 4) of the Zn-Se-Te system contains three distinct regions like many other samples (such as Cu-In-Se, As-Se-Te, CdS, etc.),[4,7,21–23] viz., the high-absorption region $h\nu>E_0$ ($\alpha>10^4$ cm^{-1}), the exponential part, and the weak-absorption tail. In the high-absorption region, the absorption coefficient α for the direct (vertical) allowed transition in the quantum-mechanical sense is given by[24–26]

$$\alpha h\nu = A(h\nu - E_0)^{1/2} . \tag{3}$$

The direct nature of the fundamental transition in $ZnSe_xTe_{1-x}$ ($0\le x\le 1$) is confirmed from the plot of $(\alpha h\nu)^2$ versus $h\nu$ shown in Fig. 5 for various compositions. From Fig. 5, the optical band gaps (E_0) are estimated for all and are shown in Fig. 6 as a function of concentration x. A distinct downward optical bowing with a minimum corresponding to x around 0.32 is observed in Fig. 6. This result agrees quite well with that of Ebina, Yamamoto, and Takahashi,[13] who obtained E_0 of these samples from reflectivity measurements with single crystals of the Zn-Se-Te system. A similar variation of

TABLE I. Some important parameters of the $ZnSe_xTe_{1-x}$ ($0\le x\le 1$) alloys. The thermal diffusivity σ and energy gap E_0 are obtained from Figs. 2 and 5, respectively. $F(m^*)$ is calculated from Eq. (6).

Sample	Thermal diffusivity σ (cm^2/sec)	E_0 (eV)	$F(m^*)$
ZnTe	1.587×10^{-2}	2.12	0.1707
$ZnSe_{0.3}Te_{0.7}$	1.547×10^{-2}	2.04	0.1643
$ZnSe_{0.8}Te_{0.2}$	1.542×10^{-2}	2.25	0.1812
ZnSe	1.604×10^{-2}	2.63	0.2118

E_0 with x was also observed from diffuse reflectance studies by Larach, Shrader, and Stocker[12] with Zn-Se-Te alloy powders. This type of variation of E_0 with x observed in Zn-Se-Te is quite different from those of ZnS_xSe_{1-x} alloys (shown in Fig. 6 for comparison). Such a variation of E_0 with x in the $ZnSe_xTe_{1-x}$ alloys can be fitted (about 98%) with an equation of the form

$$E_0(x)=2.1366-0.8399x+1.3048x^2$$

or

$$E_0(x)=E_0(0)+[E_0(1)-E_0(0)-b]x+bx^2 , \tag{4}$$

where $E_0(0)$ and $E_0(1)$ are the values of the energy gap for $x=0$ and 1, respectively, and $b=1.3048$ is the bowing parameter. The nonlinear variation of E_0 with composition x was also observed in $A^{I}B^{III}C_2^{VI}$ chalcopyrite structures by Tinoco, Quintero, and Rincon[27] and the downward bowing was explained by considering the electronegativity difference between the substituting atoms. But in the present Zn-Se-Te system the nonlinear behavior of the E_0 vs x curve (showing downward optical bowing) cannot be explained by considering the electronegativity difference[27] mentioned above. Furthermore, we also no-

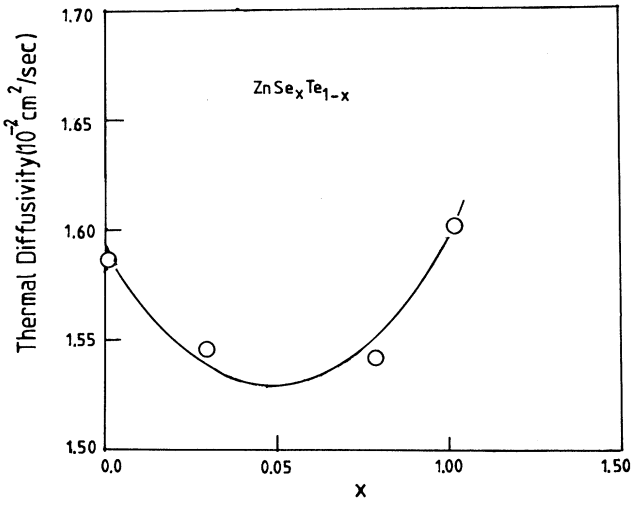

FIG. 3. Thermal diffusivity vs concentration x of the $ZnSe_xTe_{1-x}$ alloys, indicating a minimum around $x=0.48$ (solid line is the best fit of the experimental points).

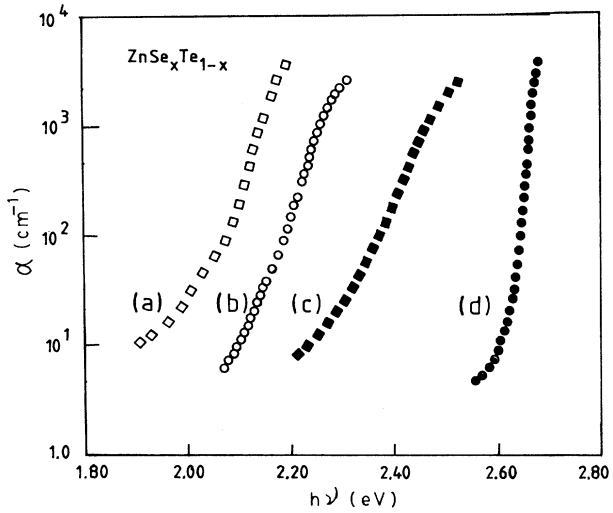

FIG. 4. Variation of the absorption coefficient α of $ZnSe_xTe_{1-x}$ as a function of the photon energy $h\nu$. Curve *a*, $ZnSe_{0.3}Te_{0.7}$, curve *b*, ZnTe, curve *c*, $ZnSe_{0.8}Te_{0.2}$, and curve *d*, ZnSe.

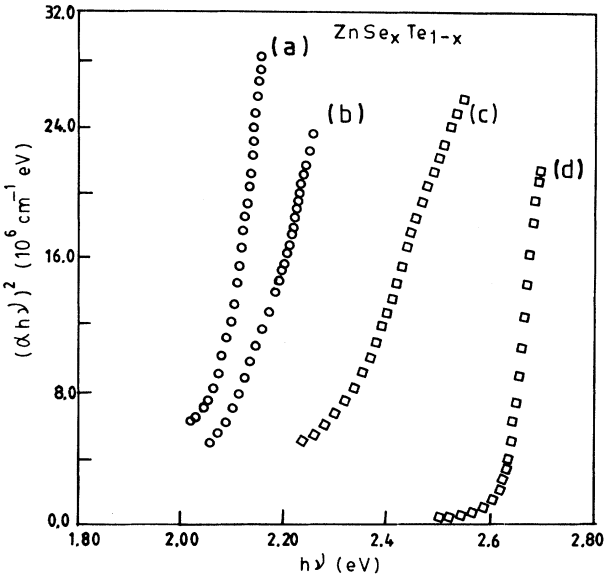

FIG. 5. Plot of $(\alpha h\nu)^2$ as a function of $h\nu$ for various concentrations x of $ZnSe_xTe_{1-x}$ alloys. Curve a, $ZnSe_{0.3}Te_{0.7}$, curve b, ZnTe, curve c, $ZnSe_{0.8}Te_{0.2}$, and curve d, ZnSe.

tice that other than electronegativity difference[27] (dotted curve in Fig. 6) additional factors arising from disorder, etc., as suggested by Bernard and Zunger,[14] are involved in these alloys. Hill and Richardson,[28] however, pointed out that in ZnS_xTe_{1-x} films, which also behave like the Zn-Se-Te system,[12] exact fitting with Eq. (4) is difficult and a cubic term (dx^3) should be included in Eq. (4) [that is, $E_0(x)=a+bx+cx^2+dx^3$]. Thus the presence of a

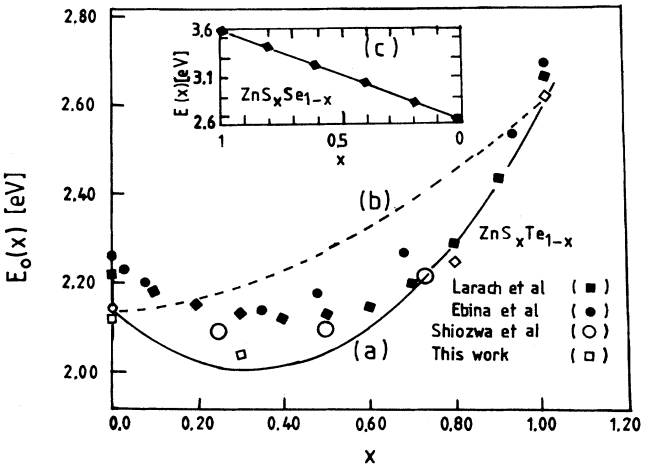

FIG. 6. Energy gap estimated from Fig. 5 is shown as a function of concentration x, indicating an optical downward bowing. The solid line (curve a) indicates the best fit to the present experimental data of $ZnSe_xTe_{1-x}$ (□) with Eq. (4). The dotted line (curve b) indicates the variation of $E_0(x)$ of $ZnSe_xTe_{1-x}$ calculated from consideration of the electronegativity difference between the substituting atoms Se and Te (Ref. 22). The inset indicates the variation of E_0 with x for ZnS_xSe_{1-x} samples (Ref. 8) shown for comparison with curve a of this figure.

cubic term in Eq. (4) seems to be important. This term might be associated with microscopic disorder in the structure and the anharmonicity effect arising from strong electron-phonon interaction terms which is considered to be important in other similar systems.[29] Our results also indicate the importance of the cubic term for a 100% fitting of the E_0 versus x curve.

B. Band-edge effective mass

We have also attempted to calculate the band-edge effective mass (m_e^*) of the carriers for the Zn-Se-Te system from our present PAS studies using the expression[30]

$$m/m_e^* = 1/m^* = 1+p^2/2mE_0$$

or

$$E_0 = p^2/2m[m^*/1-m^*] \quad (5)$$

$$= (p^2/2m)F(m^*) , \quad (6)$$

where m is the free-electron mass and p is the momentum matrix and can be expressed as $\hbar R$, where R is the smallest reciprocal lattice vector, so that $p=\hbar/a$, a being the lattice constant. From Eqs. (6) and (4) we can write

$$F(m^*,x)=F(m_0^*)+[F(m_1^*)-F(m_0^*)-b_1]x+b_1x^2 , \quad (7)$$

where $b_1=b/(p^2/2m)$, obtained by comparing Eqs. (4) and (7), and m_0^* and m_1^* correspond to the effective-mass ratios of the material with $x=0$ and $x=1$, respectively. Therefore the function $F(m^*)$ and hence $m^*(x)$ of the ternary compound semiconductors, as shown in Table I, should show a bowing behavior with the polynomial of Eq. (7). The concentration-dependent $F(m^*)$ shown in Fig. 7 clearly indicates the bowing behavior for

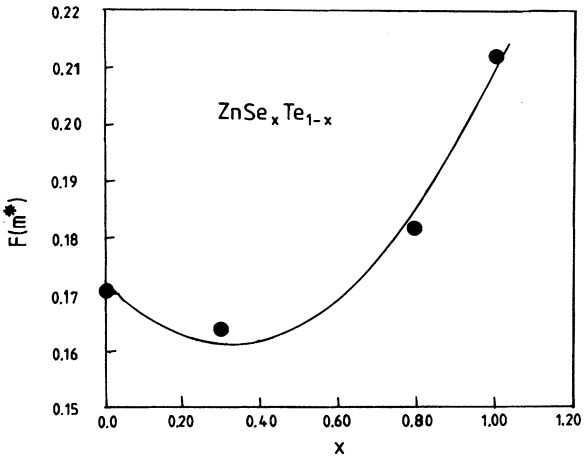

FIG. 7. The concentration (x) dependence of $F(m^*)$, indicating the downward-bowing behavior similar to that of $E_0(x)$ shown in Fig. 6. The points (●) are calculated from the experimental $E_0(x)$ values using Eq. (6) and the solid line is the best fit to those points with the polynomial $F(m^*)=0.172-0.676x+1.105x^2$.

$b_1=0.1050$, which gives $b=1.3046$ This value is very close to the value of b obtained from Eq. (4). From Fig. 7 it is evident that the variation of $F(m^*)$ with the concentration x is similar to that of E_0 with the concentration. Since both m^* and $F(m^*)$ behave in a similar fashion, calculation of $F(m^*)$ and m^* is made on the assumption that the momentum matrix p remains constant for all the $ZnSe_xTe_{1-x}$ alloys having similar band structures.[12] Thus, knowing the effective masses of the carriers (from Ref. 31), the values of $p^2/2m$ are calculated for ZnSe and ZnTe (the end-member alloys of our present investigation). The values of $p^2/2m$ for ZnSe and ZnTe (using[31] $m^*=0.17$ and 0.15, respectively, for ZnSe and ZnTe) are found to be 12.84 (for ZnSe) and 12.01 (for ZnTe), which are very close to each other. Therefore consideration of an average value of $p^2/2m$ for these alloys (Zn-Se-Te) in the above calculations seems to be reasonably justified.

C. Exponential edge

From the variation of absorption coefficient α with incident photon energy $h\nu$ as shown in Fig. 4, the exponential edge (Urbach edge) is also observed for our samples. The absorption coefficient α in this region can be written[24–26] as

$$\alpha=\alpha_0\exp\{\gamma[h\nu-E_0(T)]/k_BT^*\} \quad \text{for } h\nu<E_0(T) . \tag{8}$$

Here α_0 and γ (the order of magnitude is unity) are constants. $E_0(T)$ is the temperature-dependent gap and T^* is the effective temperature,[32] which is almost constant below a critical value T_0 and is proportional to T at high temperatures (above T_0). From Eq. (8) one finds Urbach's rule,[33] viz., $d(\ln\alpha)/d(h\nu)=\gamma/k_BT^*$, which suggests that the sharp absorption edge becomes broader as the temperature rises above T_0. This region is strongly related to structural properties of the sample and can be correlated with the impurity concentrations of the samples.[24] Recently, it has been pointed out[34–36] that γ varies linearly with temperature so that the ratio γ/k_BT^* is constant for amorphous and polycrystalline materials and it is temperature dependent for pure single crystals.

Here we would like to point out that the perturbation of the band edge may arise from intrinsic charged impurities. Such a perturbation may produce a local electric field[24] which is very large, $\sim 10^5$ V/cm. The relation between the local internal field and the Franz-Keldysh effect was shown by Dow and Redfield[37,38] who proposed that the fluctuation of the internal field was responsible for the exponential band edge,[25] as also observed in our samples studied by the photoacoustic technique.

D. Absorption tail

The tail in the absorption spectrum close to the band edge observed from this experiment is associated with phonon-assisted transitions. Its strength and shape depend on the preparation, purity, thermal history,[39] and also on the thickness of the samples.[26]

In the region $h\nu<E_0$ the dependence of α on $h\nu$ obeys[24,25] the following relation for the $ZnSe_xTe_{1-x}$ samples (except ZnTe):

$$\alpha=A'[h\nu-E_{0i}+E_p]^2/\exp(E_p/k_BT-1) , \tag{9}$$

where A' is a constant nearly independent of photon energy, T is the absolute temperature, and k_B is the Boltzmann constant. E_p and E_{0i} are, respectively, the phonon energy and optical energy gap for the indirect transition [obtained from the extrapolation of the linear portion of $\alpha^{1/2}$ vs $h\nu$ plot (Fig. 8) to the energy axis where $\alpha=0$]. The value of the phonon energy E_p is obtained from the above relation [Eq. (9)] such that $E_p=E_{0i}-h\nu$ at $\alpha=0$ (Fig. 8). The extrapolation of the linear portion to $\alpha=0$ for ZnSe gives energies of 25, 75, and 120 meV corresponding to optical phonon wave numbers 201, 604, and 967 cm^{-1}, respectively. In the case of $ZnSe_{0.3}Te_{0.7}$ these energies are found to be 65 and 75 meV which correspond to the optical phonon wave numbers 524 and 604 cm^{-1}. For the case of $ZnSe_{0.8}Te_{0.2}$ and ZnTe no specific phonon-assisted transition is obtained. The reason for this behavior is not yet clear and it needs further investigations. A similar phonon-assisted transition has also been observed in the $CuIn_xGa_{1-x}Se_2$ system using the photoacoustic technique.[4]

IV. SUMMARY AND CONCLUSION

From photoacoustic studies we have directly determined the optical energy gap E_0 and other optical properties of both $ZnSe_xTe_{1-x}$ and ZnS_xTe_{1-x} (not reported in this paper) polycrystalline alloys. The present results agree quite with those obtained by using other spec-

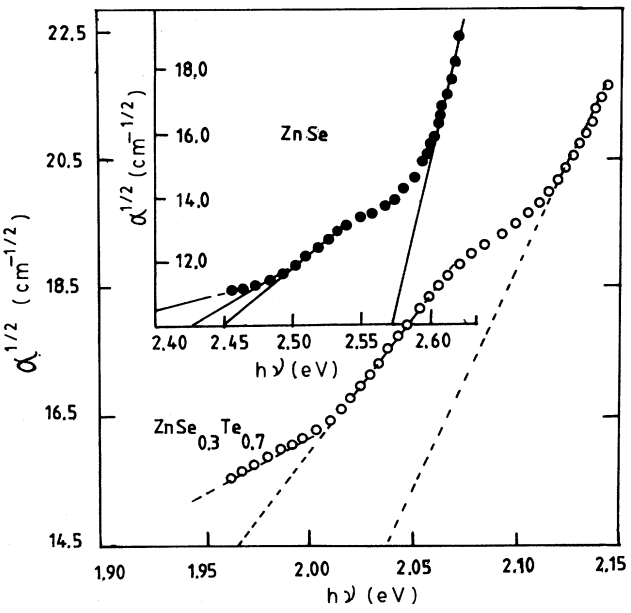

FIG. 8. Variation of $\alpha^{1/2}$ [Eq. (9)] as a function of $h\nu$ for two samples, ZnSe and $ZnSe_{0.3}Te_{0.7}$. The assisted phonon energy is calculated from this curve (see text).

troscopic techniques for single crystals and thin films. A direct determination of the thermal diffusivity σ has also been made possible from the present PAS study of these samples which has not been determined earlier by other spectroscopic techniques. It should be noted here that, though the measured values of the thermal diffusivity σ for the polycrystalline Zn-Se-Te alloys determined from the present PAS studies are comparable to those of other similar materials,[17,21] these values may differ very slightly from the corresponding values of single crystals. However, this difference has little effect on the values of the band gaps and other parameters of these alloys measured by the PAS technique as shown in the present paper. The general trends of variation of energy gap, thermal diffusivity, etc. with visible light frequency, however, remain unaltered in single crystals, alloys, and also thin films. Recently we have observed from the PAS studies that there is very little difference in the values of E_0 and thermal diffusivity obtained for glassy Ge-S(Te)-Se and polycrystalline alloys (prepared similarly to our present Zn-Se-Te alloys) of these compounds.

The variation of the optical gap shows an interesting optical downward bowing with a minima at a particular concentration ($x \sim 0.32$ for $ZnSe_xTe_{1-x}$). Though this type of nonlinear behavior in chalcopyrite and some other systems[27] could be explained by considering the electronegativity difference between the substituting atoms, this analysis is not applicable for the Zn-Se(S)-Te systems. At present no adequate theoretical analysis is available for uniquely explaining the nonlinear behavior of all such systems. The optical downward bowing is explained by Bernard and Zunger's model[14] by considering joint contributions of the order effect (estimated by the virtual-crystal approximation) and the disorder effect (estimated by the cluster-averaging method). This method also seems to be not uniquely applicable for all the systems mentioned above.

Thus, from the analysis of the PAS spectra, interesting information about the optical-absorption coefficient, thermal diffusivity, band-edge effective masses, band edge, band tail, etc. has been obtained for the Zn-Se-Te system. Finally, it is concluded that the present experimental procedure and the mode of theoretical analysis of the PAS data made for the Zn-Se-Te system could easily be extended to many other systems like solar-energy-related materials (especially for the determination of the defect states at the sub-band-gap regions), the glassy Ge-S(Te)-Se system, many dilute magnetic semiconductors, and other materials (both crystalline and glassy materials) of current technological importance.

ACKNOWLEDGMENTS

One of the authors (A.K.G.) is grateful to the University Grant Commission (Government of India) for financial support. The authors are also grateful to the Department of Science and Technology for the financial assistance to set up the photoacoustic spectrometer.

[1]A. Rosencwaig, *Photoacoustics and Photoacoustic Spectroscopy* (Wiley, New York, 1980); *Optoacoustic Spectroscopy and Detection,* edited by Y. H. Pao (Academic, New York, 1977).

[2]*Photoacoustic and Thermal Wave Phenomena in Semiconductors,* edited by A. Mandelis (North-Holland, New York, 1987); A. C. Tam, Rev. Mod. Phys. **58**, 381 (1986).

[3]V. P. Zharov and V. S. Letokhov, *Laser Optoacoustic Spectroscopy,* Springer Series in Optical Science Vol. 37 (Springer, Berlin, 1986).

[4]A. Zegadi, M. A. Slifkin, M. Djamin, A. E. Hill, and R. D. Tomlinson, Phys. Status Solidi A **133**, 533 (1992).

[5]D. Cahen, Appl. Phys. Lett. **33**, 810 (1978).

[6]S. Yamasaki, Philos. Mag. B **56**, 79 (1987).

[7]R. Kuhnert and R. Helbig, Appl. Opt. **20**, 4149 (1981); O. Zelaya-Angel, J. J. Alvarado-Gil, R. Lozada-Morales, H. Vargas, and A. Ferreira da Silva, Appl. Phys. Lett. **64**, 291 (1994).

[8]M. Aven, Appl. Phys. Lett. **7**, 146 (1965).

[9]M. Aven and W. Garwacki, J. Appl. Phys. **38**, 2302 (1967).

[10]F. F. Morehead and G. Mandel, Appl. Phys. Lett. **5**, 53 (1964).

[11]B. L. Crowder, F. F. Morehead, and P. R. Wagner, Appl. Phys. Lett. **8**, 148 (1966).

[12]S. Larach, R. E. Shrader, and D. F. Stocker, Phys. Rev. **108**, 587 (1957).

[13]A. Ebina, M. Yamamoto, and T. Takahashi, Phys. Rev. B **6** (10), 3786 (1972).

[14]J. E. Bernard and A. Zunger, Phys. Rev. B **36**, 3199 (1987).

[15]S. Adachi and T. Taguchi, Phys. Rev. B **43**, 9569 (1991).

[16]G. Ziegler and D. P. H. Hasselman, J. Mater. Sci. **16**, 495 (1981).

[17]J. C. de Lima, N. Cella, L. C. M. Miranda, C. Chying An, A. H. Franzan, and N. F. Leite, Phys. Rev. B **46**, 14 186 (1992).

[18]B. K. Chaudhuri, Indian J. Phys. **66A**, 713 (1992); J. Isaac, J. Philip, and B. K. Chaudhuri, Pramana **31**, L153 (1988).

[19]P. Poulet, J. Chambron, and R. Unterreiner, J. Appl. Phys. **51**, 1738 (1980).

[20]A. Lachaine and P. Poulet, Appl. Phys. Lett. **45**, 953 (1984); P. Charpentier, F. Lepoutre, and L. Bertrand, J. Appl. Phys. **53**, 608 (1982).

[21]K. Nandakumar and J. Philip, J. Non-Cryst. Solids **144**, 247 (1992).

[22]B. L. Evans and P. A. Young, Proc. R. Soc. London Ser. A **297**, 230 (1967).

[23]A. A. El-Shazly, H. T. El-Shair, and M. K. El-Mously, Thin Solid Films **78**, 295 (1981).

[24]J. I. Pankove, *Optical Processes in Semiconductors* (Dover, New York, 1975).

[25]N. F. Mott and E. A. Davis, *Electronic Processes in Non-Crystalline Materials* (Clarendon, Oxford, 1979).

[26]J. Tauc, in *Amorphous and Liquid Semiconductors,* edited by J. Tauc (Plenum, New York, 1974), Chap. 4.

[27]T. Tinoco, M. Quintero, and C. Rincon, Phys. Rev. B **44**, 1613 (1991).

[28]R. Hill and D. Richardson, J. Phys. C **6**, L115 (1973).

[29]W. J. Daughton and B. DeFacio, J. Phys. C **11**, 4307 (1978).

[30]D. K. Ferry, *Semiconductors* (Macmillan, New York, 1991), Chap. 5.

[31]Brian Roy, *II-IV Compounds,* 1st ed. (Pergamon, Oxford, 1969).

[32]H. Mahr, Phys. Rev. **132**, 1880 (1963).

[33]F. Urbach, Phys. Rev. **92**, 1324 (1953).
[34]L. Samuel, Y. Brada, A. Burger, and M. Roth, Phys. Rev. B **36**, 1168 (1987).
[35]L. Samuel, Y. Brada, and R. Beserman, Phys. Rev. B **37**, 4671 (1988).
[36]M. Neumann-Spallart, E. Galun, G. Hodes, C. Levy-Clement, Y. Marfaing, E. Muranevich, and R. Tenne, J. Appl. Phys. **73**, 7753 (1993).
[37]D. Redfield, Phys. Rev. **130**, 916 (1963).
[38]J. D. Dow and D. Redfield, Phys. Rev. B **1**, 3358 (1970).
[39]A. Vasco, D. Lezal, and I. Srb, J. Non-Cryst. Solids **4**, 311 (1970).